

Numerical Simulation of Natural Convection in a Square Cavity Utilizing Nanofluid and Subjected to Air Stream Cooling

Khalid B. Saleem

Mech. Eng. Department

Engineering College

University of Basrah

khalid.saleem@uobasrah.edu.iq;khalidb77@gmail.com

Abstract-In the present paper the natural convection in a square cavity utilizing Cu-water nanofluid is examined numerically. The cavity is exposed to cooling air stream with free stream temperature (T_∞) from left wall and its right and bottom walls kept with cold and hot temperatures (T_C) and (T_H) respectively, while the cavity top wall considered as adiabatic. The nanofluid flow inside the cavity is assumed to be laminar and obeying to Boussinesq approximation. The governing equations are solved by finite volume method using ANSYS FLUENT code. The results are accomplished with a range of nanofluid volume fraction $\phi=0-0.16$, Rayleigh number $Ra=10^3-10^5$ and free stream Reynolds number $Re_\infty=10^3-10^4$. The effects of these variables are displayed on the stream function (ψ), isotherms (θ) contours and average Nusselt number (Nu_{avg}). The results show the heat transfer rate augmented with increasing ϕ , Ra and Re_∞ . Also, the increment in both ϕ and Ra increases the circulation inside the cavity while increasing Re_∞ produces secondary vortices and reduces circulation at the main vortex of the cavity. The results of local Nusselt number (Nu) and isotherms (θ) are compared with other studies and show good agreement with maximum error values 14.28% and 3.2% respectively.

Index Terms- *Natural convection; Square cavity; Nanofluid; Air stream cooling; Finite volume.*

I. INTRODUCTION

The flow inside cavities is a most common phenomenon handled in many numerical simulations. Most studies focused in improving heat transfer rate within the cavity and using different ways to fulfill this thing, some of these ways related to the design of the cavity and some of it use various fluids other than air or water inside the cavity like nanofluids. Nanofluids are fluids consisting from nanometer-sized particles known as nanoparticles and have a variety of applications in industry, such as electronic devices [1], heat exchangers [2], coolants in automobiles [3], refrigeration systems [4] and manufacturing processes [5].

Several authors investigated the flow of nanofluids inside cavities in their studies. Manab and Pravin [6]

conducted the performance of nanofluids within a square cavity which partly heated and cooled to get understanding into heat transfer and flow methods. They employed the finite volume technique with SIMPLEC algorithm to resolve the governing equations numerically. Their investigation concentrates on the study of many factors on the heat transfer features of nanofluids inside the cavity like Grashof number, nanoparticle volume fraction and position of the active walls. Their results show that the fluid movement and heat transmission were affected by the Grashof number and volume fraction concentration. Jahanshahi et al. [7] analyzed numerically the flow in a square cavity exposed to various sidewall temperatures utilizing water/SiO₂ nanofluid. They anticipated the thermal conductivity of nanofluid from experimental results and implement for it various relations. The results achieved with numerous magnitudes of Rayleigh number and volume content of nanoparticle. Their results demonstrated the mean Nusselt number was augmented with increases volume content for all the attempted scopes of Rayleigh number. Sheikhzadeh et al. [8] simulated numerically the buoyancy flow and heat transfer in a square enclosure with partly dynamic sidewalls loaded with Cu-water nanofluid. They inspected different parameters on its influence upon fluid motion and heat transmission within the domain such as Rayleigh number, the positions of the dynamic portions of the side walls and the percentage volume content of the solid nanoparticles. They found that the mean Nusselt number improves by expanding each of the Rayleigh number and solid nanoparticles percentage content.

Abbasian et al. [9] examined numerically the mixed convection flow of Cu-water nanofluid within a square lid-driven enclosure with adiabatic horizontal walls and the sidewalls heated with a sinusoidal temperature profile. Their results indicated that for a fixed Grashof number, the forced convection heat transfer become stronger with diminish in Richardson number and the heat transmission is controlled by natural convection when constant Reynolds number was considered. Rahmati et al. [10] considered the heat transfer behavior in a cavity containing nanofluids. They used lattice Boltzmann procedure for solving the velocity field and simulate heat transfer utilizing single-relaxation-time lattice

Boltzmann scheme, while the Boussinesq approximation is used to combine between the hydrodynamics and thermal domains. They considered the Cu-water as nanofluid and studied the impact of Grashof number and volume content on thermal and hydrodynamic features. Their result obviously presented that heat transfer improved when the volume content increases and this improvement is conceivable using nanofluids in contrast with regular liquids. Salva and Chamkha [11] examined laminar natural convection and entropy generation in an odd-shaped cavity occupied by Cu-water nanofluid. They solved the governing equations numerically by finite element scheme by means of Galerkin weighted residual technique. Their simulations based upon the effects of natural convection characteristics and volume concentration of nanoparticle on each of the mean Nusselt number, Bejan number and overall entropy generation. They predict the streamlines and isotherms for several Rayleigh number and different nanoparticles volume concentration. Their calculations demonstrated that the mean Nusselt number and the heat transfer term of entropy are improves with increasing Rayleigh number. Said et al. [12] recently exhibited a numerical analysis of free convection in a square cavity utilizing three dissimilar nanofluids (i.e., Cu, Al₂O₃ or TiO₂) with a partly heated square chunk at its center. They assumed the side walls of the outer cavity at fixed but dissimilar temperatures whereas the upper and lower walls as insulated. The finite volume procedure and SIMPLEC method are used for the simulation and the influence of related parameters like Rayleigh number, volume concentration for the nanoparticles and aspect ratio are examined. Their calculations demonstrated increment in heat transfer quantity with augmenting the solid volume content of the nanofluids and best heat transfer enhancement accomplished with copper and silver nanoparticles.

From the above literature reviews, it can be seen that there are a lot of studies using numerical methods on natural convection in square cavities utilizing nanofluids with various boundary conditions at the cavity walls, but none of these considered the cooling with free air stream. The aim of the present paper is to investigate the natural convection on a square cavity full with Cu-water nanofluid and subjected to cooling effect of external air stream from its left side. The governing equations are implemented numerically using finite volume scheme with utilizing ANSYS FLUENT code. The influence of several parameters is considered such as nanofluid volume fraction, Rayleigh number and Reynolds number for air stream. Also, the obtained results are represented by contours of stream function, isotherms and average Nusselt number plots.

II. PROBLEM DESCRIPTION AND MATHEMATICAL FORMULATION

In the present study a square two-dimensional cavity occupied with Cu-water nanofluid shown in Fig. 1 of

dimensions (L×L) is heated from the bottom wall with the hot temperature (T_H) and subjected to cooling air stream from the left wall which has free stream temperature (T_∞) and convection heat transfer coefficient (h_∞). The right cavity wall kept with the cold temperature (T_C) while the top wall of the cavity was considered as adiabatic. The flow of air outside the cavity is considered to be laminar and constant properties, while the flow of the nanofluid inside the cavity is taken as steady, incompressible, laminar and obeying to Boussinesq approximation (i.e., the density of the nanofluid varied with temperature). Furthermore, there is a thermal equilibrium between the heat transferred by conduction at the left cavity wall with the convective heat transferred from air.

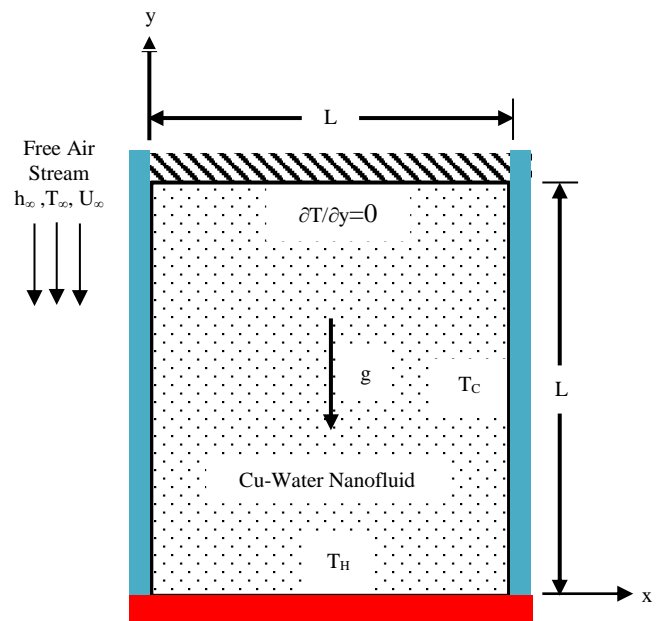


Fig. 1 Physical domain and coordinates system

The governing equations describe these conditions mentioned below.

Continuity equation:

$$u \frac{\partial u}{\partial x} + v \frac{\partial v}{\partial y} = 0 \quad (1)$$

The x-direction momentum equation is given as:

$$u \frac{\partial u}{\partial x} + v \frac{\partial u}{\partial y} = -\frac{1}{\rho_{nf}} \frac{\partial p}{\partial x} + \frac{\mu_{nf}}{\rho_{nf}} \left(\frac{\partial^2 u}{\partial x^2} + \frac{\partial^2 u}{\partial y^2} \right) \quad (2)$$

The y-direction momentum equation is:

$$u \frac{\partial v}{\partial x} + v \frac{\partial v}{\partial y} = -\frac{1}{\rho_{nf}} \frac{\partial p}{\partial y} + \frac{\mu_{nf}}{\rho_{nf}} \left(\frac{\partial^2 v}{\partial x^2} + \frac{\partial^2 v}{\partial y^2} \right) + \frac{1}{\rho_{nf}} \left[\phi \rho_s \beta_s + (1 - \phi) \rho_f \beta_f \right] g (T - T_c) \quad (3)$$

Energy equation:

$$u \frac{\partial T}{\partial x} + v \frac{\partial T}{\partial y} = \alpha_{nf} \left(\frac{\partial^2 T}{\partial x^2} + \frac{\partial^2 T}{\partial y^2} \right) \quad (4)$$

The suggested nanofluid is Cu-water its properties with air properties are shown in Table 1.

TABLE 1 THERMO-PHYSICAL PROPERTIES OF NANOFLUID AND AIR

Property	Fluid Phase (Air)	Fluid Phase (Water)	Solid Phase (Cu)
C_p (J/kg.K)	1006.3	4179	383
ρ (kg/m ³)	1.1845	997.1	8954
μ (kg/m.s)	1.844×10^{-5}	8.9×10^{-4}	-
k (W/m.K)	0.025969	0.6	400
β (1/K)	0.003354	2.1×10^{-4}	1.67×10^{-6}

The relations of the nanofluid thermo-physical properties used in Eqs. (1)-(4) can be defined as follows:

For the effective viscosity of nanofluid having a dilute abeyance of tiny unbending spherical particles the relation defined by Brinkman [13] is used:

$$\mu_{nf} = \frac{\mu_f}{(1-\phi)^{2.5}} \tag{5}$$

For the effective density of the nanofluid on related temperature the relation is [14]:

$$\rho_{nf} = (1-\phi)\rho_f + \phi\rho_s \tag{6}$$

The heat capacitance of the nanofluid ($C_{p,nf}$) and the thermal expansion coefficient (β_{nf}) are defined as given by Jang [15]:

$$(\rho C_p)_{nf} = (1-\phi)(\rho C_p)_f + \phi(\rho C_p)_s \tag{7}$$

$$(\rho\beta)_{nf} = (1-\phi)(\rho\beta)_f + \phi(\rho\beta)_s \tag{8}$$

The effective thermal conductivity of fluid can be evaluated using Maxwell-Garnett's (MG) model. For the two-component object of spherical-particle suspension, the MG model provides [16]:

$$\frac{k_{nf}}{k_f} = \frac{(k_s+2k_f)-2\phi(k_f-k_s)}{(k_s+2k_f)+\phi(k_f-k_s)} \tag{9}$$

For the specified problem, the suitable boundary conditions at the system borders are:

1- On $x = 0$, $u = v = 0$, and $k_{nf} \frac{\partial T}{\partial x} = h_{\infty}(T - T_{\infty})$ for $0 \leq y \leq L$

2- On $x = L$, $u = v = 0$, and $T = T_C$ for $0 \leq y \leq L$

3- On $y = 0$, $u = v = 0$, and $T = T_H$ for $0 \leq x \leq L$

4- On $y = L$, $u = v = 0$, and $\frac{\partial T}{\partial y} = 0$ for $0 \leq x \leq L$

where h_{∞} is the free stream average heat transfer coefficient that can be evaluated from the average Nusselt number (Nu_{∞}) relation given below for external flow of air over the cavity wall, and since the flow of air was assumed as laminar flow hence [17]:

$$Nu_{\infty} = 0.664 Re_{\infty}^{1/2} Pr_{\infty}^{1/3} \tag{10}$$

If $Nu_{\infty} = \frac{h_{\infty} L}{k_{\infty}}$ then h_{∞} will be given as:

$$h_{\infty} = 0.664 \left(\frac{k_{\infty}}{L} \right) Re_{\infty}^{1/2} Pr_{\infty}^{1/3} \tag{11}$$

The air stream Reynolds number (Re_{∞}) is estimated at the full cavity length (L) by the relation $\left(Re_{\infty} = \frac{U_{\infty} \rho_{\infty} L}{\mu_{\infty}} \right)$ while Pr_{∞} is

the prandtl number for air stream estimated as $\left(Pr_{\infty} = \frac{\mu_{\infty} C_{p,\infty}}{k_{\infty}} \right)$.

It is possible to transform the last equations into dimensionless formulas with adopting the subsequent dimensionless factors:

$$X = \frac{x}{L}, Y = \frac{y}{L}, U = \frac{u}{V_o}, V = \frac{v}{V_o}, P = \frac{p}{\rho_{nf} V_o^2},$$

$$\theta = \frac{(T-T_C)}{(T_H-T_C)}, \theta_{\infty} = \frac{(T_{\infty}-T_C)}{(T_H-T_C)}, Ra = \frac{\beta_{nf} g (T_H-T_C) L^3}{\nu_{nf} \alpha_{nf}}, V_o =$$

$$\frac{\mu_{nf}}{\rho_{nf} L}, Pr_{nf} = \frac{(\mu C_p)_{nf}}{k_{nf}}$$

The governing equations are reformulated into dimensionless form, utilizing the above associated dimensionless parameters as below:

Continuity equation:

$$\frac{\partial U}{\partial X} + \frac{\partial V}{\partial Y} = 0 \tag{12}$$

x-direction momentum equation:

$$U \frac{\partial U}{\partial X} + V \frac{\partial U}{\partial Y} = -\frac{\partial P}{\partial X} + \left(\frac{\partial^2 U}{\partial X^2} + \frac{\partial^2 U}{\partial Y^2} \right) \tag{13}$$

y-direction momentum equation:

$$U \frac{\partial V}{\partial X} + V \frac{\partial V}{\partial Y} = -\frac{\partial P}{\partial Y} + \left(\frac{\partial^2 V}{\partial X^2} + \frac{\partial^2 V}{\partial Y^2} \right) + \frac{Ra}{Pr_{nf}} \theta \tag{14}$$

Energy equation:

$$U \frac{\partial \theta}{\partial X} + V \frac{\partial \theta}{\partial Y} = \frac{1}{Pr_{nf}} \left(\frac{\partial^2 \theta}{\partial X^2} + \frac{\partial^2 \theta}{\partial Y^2} \right) \tag{15}$$

The governing equations for the present study can be altered by means of stream function (ψ) and vorticity (ω) formulation in which $U = \frac{\partial \psi}{\partial Y}$, $V = -\frac{\partial \psi}{\partial X}$ and $\omega = -\nabla^2 \psi$. So the equations can be written with considering all the previously mentioned presumptions in dimensionless form as below [18]:

Stream function equation:

$$\frac{\partial^2 \psi}{\partial X^2} + \frac{\partial^2 \psi}{\partial Y^2} = -\omega \tag{16}$$

Vorticity equation:

$$U \frac{\partial \omega}{\partial X} + V \frac{\partial \omega}{\partial Y} = \left(\frac{\partial^2 \omega}{\partial X^2} + \frac{\partial^2 \omega}{\partial Y^2} \right) + \frac{Ra}{Pr_{nf}} \frac{\partial \theta}{\partial X} \tag{17}$$

The boundary conditions can be also transformed into dimensionless form in terms of (ψ, ω) formulation using all previous assumptions, hence the boundary conditions will be in dimensionless form as below:

1- On $X = 0$, $U = V = \psi = 0$, and $\frac{\partial \theta}{\partial X} = Nu_{\infty}(\theta - \theta_{\infty})k_r$ for $0 \leq Y \leq 1$

2- On $X = 1$, $U = V = \psi = 0$, and $\theta = 0$ for $0 \leq Y \leq 1$

3- On $Y = 0$, $U = V = \psi = 0$, and $\theta = 1$ for $0 \leq X \leq 1$

4- On $Y = 1$, $U = V = \psi = 0$, and $\frac{\partial \theta}{\partial Y} = 0$ for $0 \leq X \leq 1$

Where k_r is the ratio of air conductivity to nanofluid conductivity, i.e. $k_r = k_{\infty}/k_{nf}$.

The local Nusselt number (Nu) of the nanofluid on the walls is estimated using the relation:

$$Nu = -\frac{L}{\Delta T} \frac{\partial T}{\partial y} \quad (18)$$

where ΔT is the temperature difference which is predicted as $\Delta T = (T_H - T_r)$, T_r : is the reference temperature which at the current study was considered as the average temperature between the cold and hot temperatures which calculated as $T_r = (T_H + T_C)/2$.

While the average Nusselt number (Nu_{avg}) at the bottom cavity wall is evaluated as:

$$Nu_{avg} = \frac{1}{L} \int_0^L Nu dx \quad (19)$$

III. SOLUTION PROCEDURE

The governing equations mentioned at the previous section are solved numerically by ANSYS FLUENT code with applying finite volume method. The SIMPLE algorithm is utilized to link between the momentum and the continuity equations. The pressure is discretized with PRESTO (Pressure Staggering Option) scheme and second-order upwind was chosen as interpolation scheme for both momentum and energy equations. The method of Patankar [19] is followed to obtain the solution of the discretized momentum and pressure equations. The iterative method is started by solving the momentum equations followed by energy equation and is proceeded till convergence is accomplished. The accuracy of all the dependent variables is considered as 10^{-6} .

A. Grid independency test

In order to obtain the optimum number of grid for the present model, grid independent test is implemented for a square cavity occupied by Cu-water nanofluid at $\phi=0.08$, $Ra=10^5$ and $Re_\infty=10^4$. The Nu_{avg} at the bottom cavity wall was evaluated with six grid values as illustrated in Table 2. It is clearly noticed that Nu_{avg} is increased by increasing the grid number until convergence achieved at the greater mesh number which indicates the proper number of grid reaches. Hence the number of grid is selected as 140×140 cells which it the best for the calculation and less time in run.

TABLE 2 GRID INDEPENDENCY TEST FOR Cu-WATER NANOFLUID $Ra=10^5$, $\phi=0.08$, $Re_\infty=10^4$

Grid Number	60×60	80×80	100×100	120×120	140×140	160×160
Nu_{avg} (Eq. 19)	8.597	8.802	8.963	9.094	9.12	9.12

B. Model validation

The validity of the current model is confirmed with the calculations of two different cases from other authors as

revealed in Figs. 2–4. In Fig. 2 ψ and θ contours predicted by configuring the present model with the same case conditions given by Sathiyamoorthy et al. [20] for a square cavity with diversely heated side walls and filled with air at $Ra=10^5$ and $Pr=0.715$. It is seen from the figure that the results shows same behavior of ψ contours at the two methods of prediction and the values of ψ look close to each other. Same behavior can be observed for θ which look in a very good agreement with Sathiyamoorthy et al. [20] results that indicates the validity of the present model in studying the natural convection inside a square cavity.

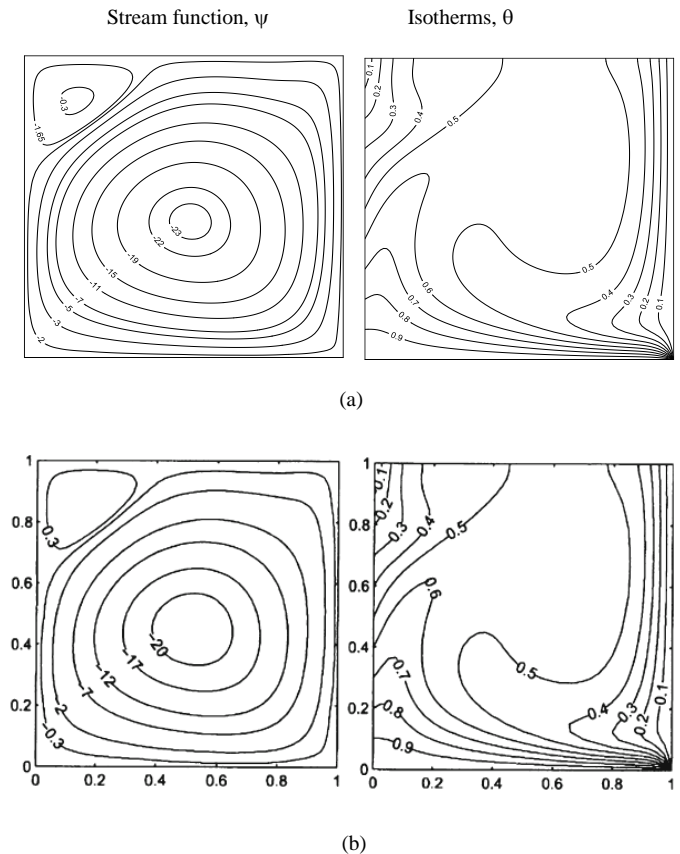


Fig. 2 Comparison of stream function and isotherms contours for air at $Ra=10^5$ between (a) the present study and (b) Sathiyamoorthy et al. [20] results

In Fig. 3 Nu on the lower wall of cavity is compared with that evaluated from Sathiyamoorthy et al. [20] model, it is obviously noticed from the figure that Nu values estimated from the present model coincide with that obtained from Sathiyamoorthy et al. [20] model in most points along the lower cavity wall and the maximum error is estimated as 14.28%. In Fig. 4 the isotherms at mid plane of a square cavity occupied with Cu-water nanofluid at $\phi=0.1$, $Gr=10^4$ (where Gr is the Grashof number ($Gr = \frac{\beta n f g (T_H - T_C) L^3}{\nu n f^2}$)) and $Pr_{nf}=3.3$, was matched with the results of Khanafer et al. [16] under the same conditions. It is shown from the figure that the present model results are quite fit with Khanafer et al. [16] results with maximum error 3.2% which demonstrate the validity of the present study.

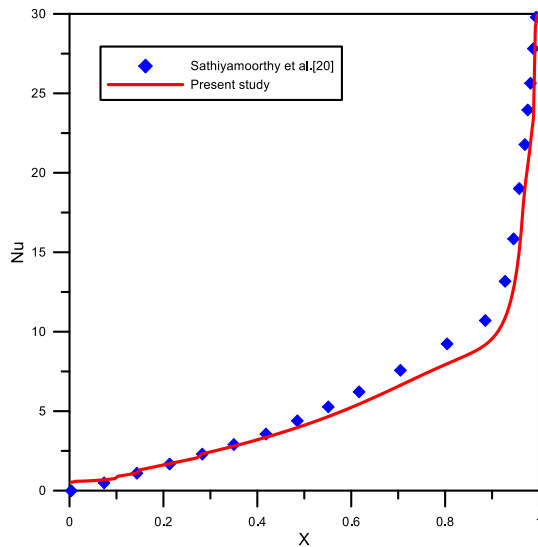


Fig. 3 Comparison between present model and Sathiyamoorthy et al. [20] results for local Nusselt number at the bottom wall of a square cavity filled with air at $Ra=10^5$, $Pr=0.715$

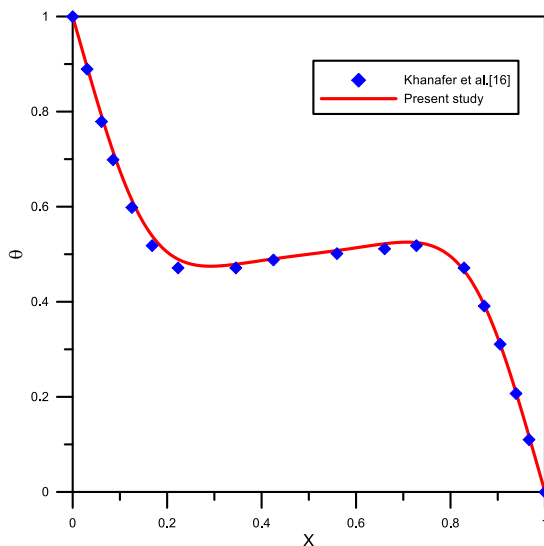


Fig. 4 Isotherms comparison between present study with Khanafer et al. [16] case for Cu-water nanofluid at $Gr=10^4$, $\phi=0.1$, $Pr_{nf}=3.3$

IV. RESULTS AND DISCUSSION

In the current analysis the calculations are carried out with several values of $Ra=10^3-10^5$, $Re_\infty=10^3-10^4$ and $\phi=0-0.16$ with $Pr_\infty=0.715$. The effect of these variables on ψ , θ and Nu_{avg} is discussed and analyzed separately in the next sections.

1. Effect of Rayleigh number

The contours of ψ and θ are plotted in Figs. 5–7 with three different values of $Ra=(10^3,10^4,10^5)$, five values of $\phi=(0-0.16)$ and constant $Re_\infty=10^4$.

In Fig. 5 for all the attempted values of ϕ with $Ra=10^3$ it is clearly seen that there are three vortices occupied the cavity, one big (the main vortex) lies in the center and right side of the cavity and two secondary vortices lie to the left side of the cavity. The secondary vortices formed due to increase rate of convection from air on the left side of cavity (due to higher Re_∞) and the buoyancy will be less in this case due to low Ra (i.e., $Ra=10^3$). The higher convection effect of air in this case forces the main vortex to be shifted to the right portion of the cavity. The isotherms at the same figure appear varying smoothly from the left wall and their values increase vertically towards the bottom (hot) wall and decrease towards the top wall. This behavior usually refers to the fact that the liquid located at the lower part of the cavity is hotter (due to it being nearest to the hot wall) than the liquid at the upper part (due to reduction in temperature when moving vertically upward). It is seen also that the lines of θ collected at the right bottom corner of the cavity and forms a singularity.

Fig. 6 show for $Ra=10^4$ that the main vortex in the cavity moves to the left and its size increases due to increasing buoyancy and this leads to decrease the size of the secondary vortex on the left bottom corner and the other secondary vortex on the top left corner moved towards the left cavity wall. This behavior shows that when Ra increases the temperature variance between the hot and cooled walls in the cavity will increase, this leads the hot liquid at the mid of cavity transfer towards the left side of the cavity. Furthermore, the tendency of ψ increases as a result of increasing buoyancy which means more circulation will happen in the cavity when compared with the cases in Fig. 5. For the isotherms when Ra increases, θ will spread significantly towards the upper wall of the cavity and changed greatly. Moreover the gradient of θ at the lower wall increases that means increasing the heat transfer at this portion of the cavity.

In Fig. 7 when $Ra=10^5$ the buoyancy effect will be larger and become more clear on the cavity and there are just two vortices occupied the cavity, the larger main vortex which grow significantly and occupy nearly 80% of cavity space while the upper left corner of the cavity still occupied by the secondary vortex due to higher cooling at this portion of the cavity. The figure also shows that the circulation at the main vortex is more pronounced with increasing Ra and this indicator of increase the tendency of ψ to higher values when compared with the previous two cases with lesser Ra . The isotherms are more shifted towards the top of the cavity and their gradients increase showing more enhancing in heat transfer rate. In addition to that, the isotherms look near the right (cold) wall as straight lines and this refers to the liquid closest to the right wall is cold.

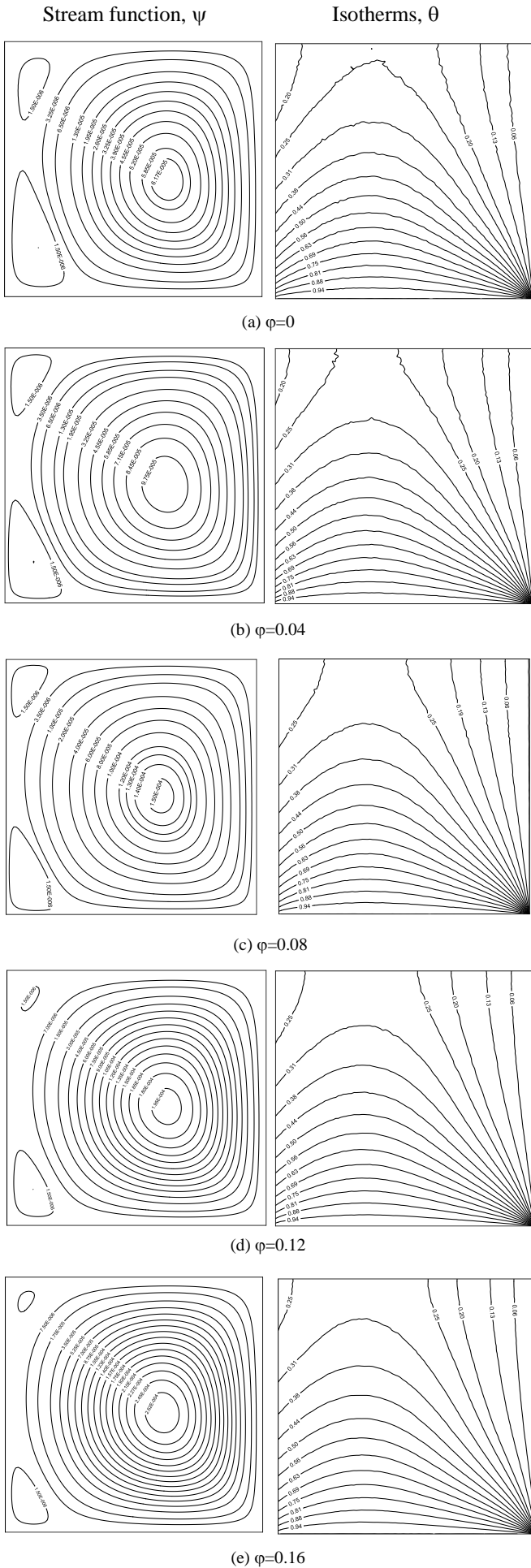


Fig. 5 Stream function and isotherms contours for various Cu-water nanofluid volume fraction with $Ra=10^3$ and $Re_c=10^4$

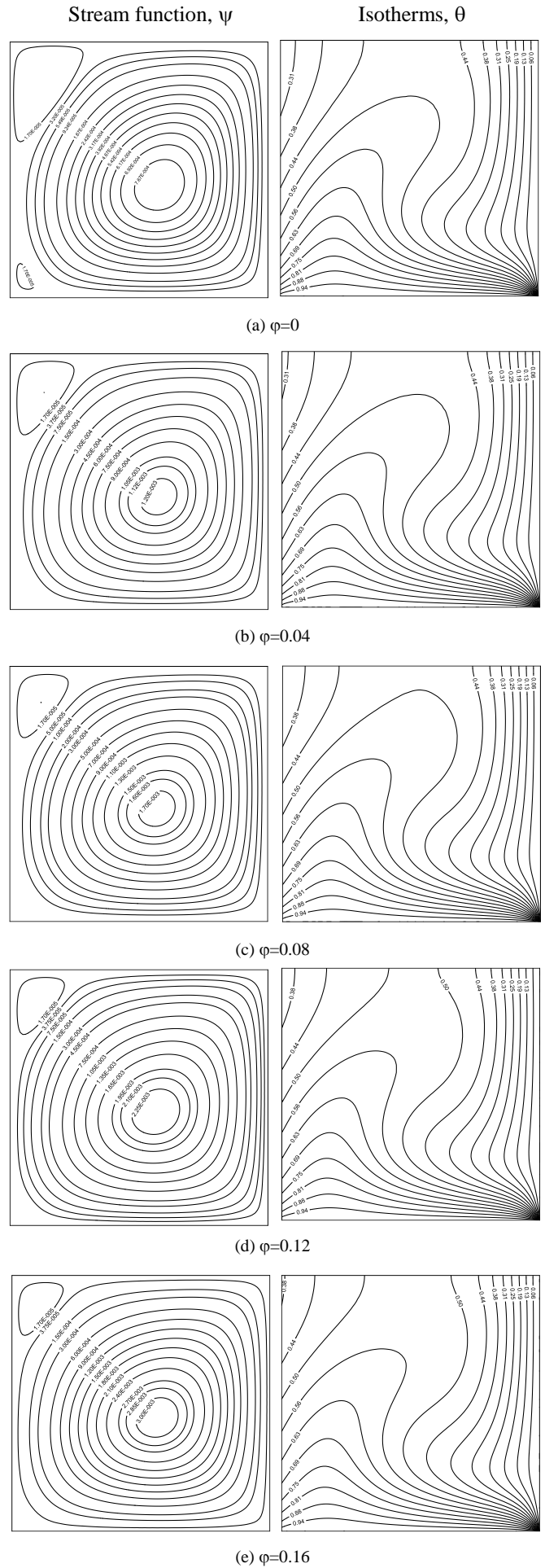


Fig. 6 Stream function and isotherms contours for various Cu-water nanofluid volume fraction with $Ra=10^4$ and $Re_c=10^4$

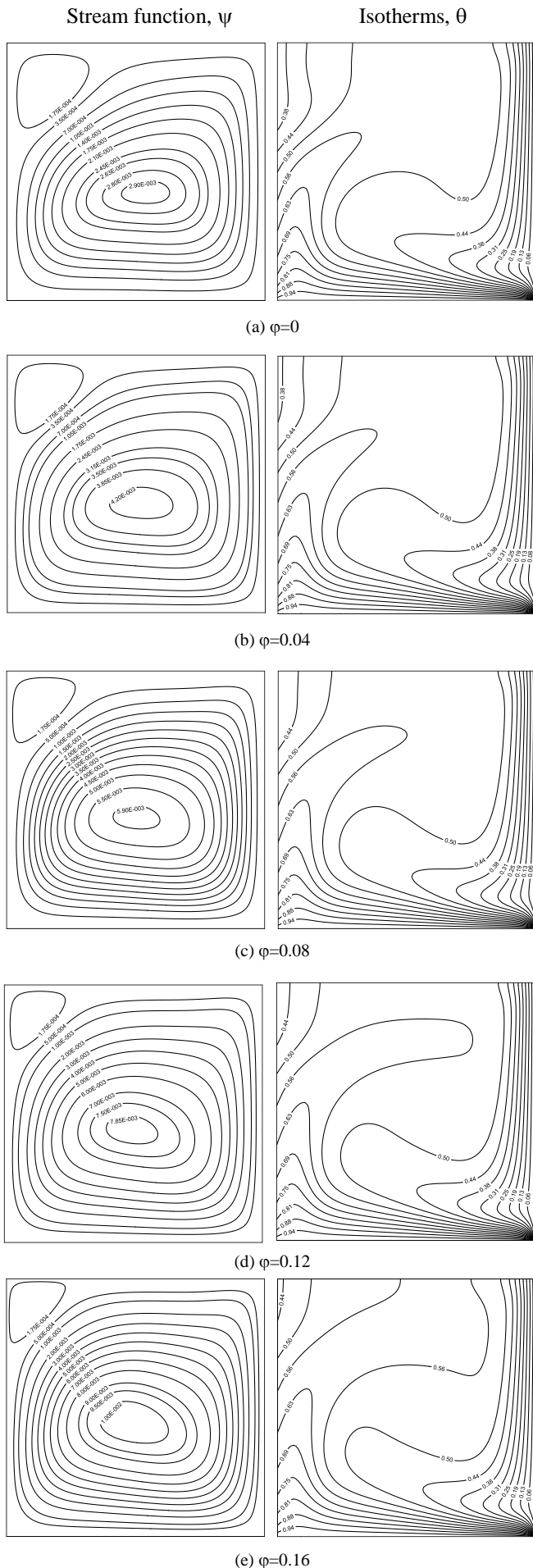


Fig. 7 Stream function and isotherms contours for various Cu-water nanofluid volume fraction with $Ra=10^5$ and $Re_\infty=10^4$

2. Effect of nanofluid volume fraction

The influence of Cu-water volume fraction is studied with five values of $\phi=(0,0.04,0.08,0.12,0.16)$, three values of $Ra=(10^3-10^5)$ and $Re_\infty=10^4$ as revealed in Figs. 5–7. Figs. 5a–5e show ψ and θ contours for $Ra=10^3$, in Fig. 5a for pure water (i.e., at $\phi=0$) it clearly seen that the buoyancy is less than the convection exerted on the left wall of the cavity (due to higher $Re_\infty=10^4$) which leads then to create two secondary vortices that appear clearly in that side. At the other Figs. 5b–5e when ϕ increases, the circulation on the middle (main) vortex increases and make it move to the left due to increase the buoyancy driven flow which leading to decrease the size of the secondary vortices on the left side of the cavity. For the isotherms, the effect of varying ϕ can be noticed with tracking one of the contours level through all the attempted ϕ values. It is observed that the contour level with ($\theta=0.25$) moves gradually to the upper left corner of the cavity with augmenting ϕ until it completely becomes at the top left corner with the largest ϕ (i.e., when $\phi=0.16$) and this belongs to increment in thermal diffusivity of the nanofluid with increasing ϕ . The figures also show that there is a little increment on the gradient of θ on the lower hot wall which an indicator to increase the heat transfer rate at this portion.

Figs. 6a–6e show ψ and θ for $Ra=10^4$. The figures reveal that the ψ tendency increases with increasing ϕ and this refers to the fact that when ϕ increases the buoyancy effect will be large then circulation will increase leading the main vortex in the cavity expands towards the lower left corner of the cavity as shown in Fig. 6c for $\phi=0.08$. Also when ϕ increases to higher values (i.e., $\phi=0.12-0.16$) as shown in Figs. 6d–6e, the main vortex expands towards the upper left corner then leading to compress the secondary vortex that existing in that region reducing its size at this part of the cavity. The isotherms behavior in Figs. 6a–6e can be understood with tracking the isotherm with ($\theta=0.5$), this value of contour level seen to be moved firstly towards the top of the cavity for pure water and lower range of ϕ (i.e., $\phi=0-0.08$), and as ϕ increases to higher values (i.e., $\phi=0.12-0.16$) this contour level will transfers to the left upper corner of the cavity leading the gradient of θ in the upper segment of the left cavity wall to increase.

Figs. 7a–7e for $Ra=10^5$ illustrate that with increasing ϕ the tendency of ψ more increases that means additional movement on the fluid inside the cavity will happen due to increases buoyancy. This will leads to force the central vortex on the cavity spans and occupy more space. For the isotherms, it is can be seen from the figures that it highly affected with increasing ϕ to higher values (i.e., with $\phi=0.08-0.16$) and this can be seen clearly with tracking isotherm line with ($\theta=0.56$) at all Figs. 7a–7e. Also, the temperature gradient of the lines becomes more pronounced with increasing ϕ which showing improvement in heat transfer rate.

3. Effect of free stream Reynolds number

Figs. 8a–8c illustrate the contours of ψ and θ with three values of $Re_\infty=(1000, 5000, 10000)$ with $Ra=10^3$ and $\phi=0.08$. In Fig. 8a it can be noticed that there is only one central vortex occupies most of cavity space and this refers to less convection exerted from the left wall (as a result to lower Re_∞). In Fig. 8b and Fig. 8c as Re_∞ increases, the heat transfer coefficient (h_∞) (i.e., predicted from Eq. (11)) will increase which leads to increasing the rate of cooling that become higher than buoyancy (as long as Ra kept fixed) within the cavity. Consequently, the intensity of ψ will decrease and the liquid will become heavier due to increasing density with reducing the temperature at the larger part of the cavity.

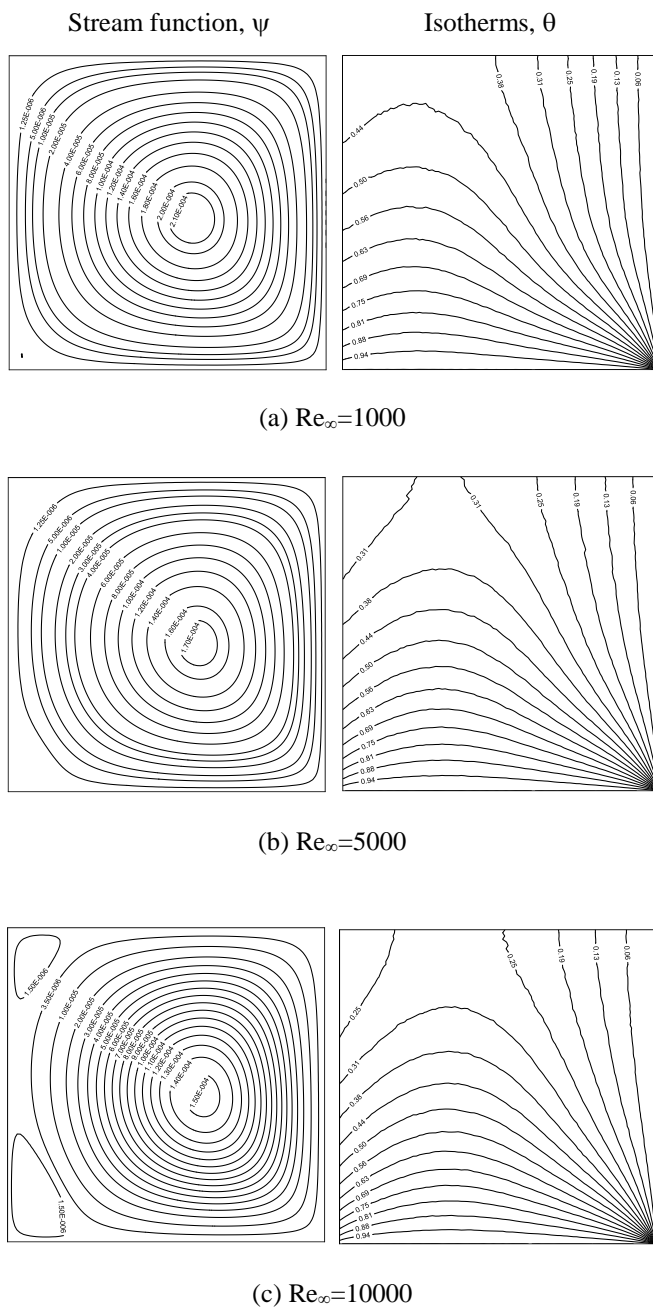


Fig. 8 Stream function and isotherms contours for Cu-water nanofluid with various air stream Reynolds number at $\phi=0.08$ and $Ra=10^3$ Furthermore, secondary vortices will be formed when Re_∞ increases due to higher cooling inside the cavity especially

near the left wall which more affected when compared to other cavity walls because it nearest to the cooling fluid. For the isotherms, when Re_∞ increases θ will be closer to the hot bottom wall due to increasing the rate of cooling from the left cavity wall and this will improving the natural convection within the cavity which making the liquid inside the cavity be colder therefore the temperature difference from top left wall will decreases.

4. Effect of nanofluid volume fraction and free stream Reynolds number on average Nusselt number

The effect of ϕ on Nu_{avg} on the lower cavity wall is shown in Fig. 9 for three different $Ra=(10^3, 10^4, 10^5)$ at $Re_\infty = 10^4$. As shown in the figure, for each value of Ra as ϕ increases Nu_{avg} will increases, the percentage increment of heat transfer rate between $\phi=0$ and $\phi=0.16$ for $Ra=10^3$ is 19.79% and it rises to 30.67% at the largest Rayleigh (i.e. $Ra=10^5$) which indicates augmentation in heat transfer rate within the cavity. Also with increasing Ra for each single ϕ value the Nu_{avg} increases and the increment between $Ra=10^3$ and $Ra=10^5$ is 83.48% at $\phi=0.16$, this reflected to increase of buoyancy driven flow as a consequence of large temperature variance among the cavity walls.

Fig. 10 reveals the change of Nu_{avg} on the bottom wall of cavity against a range of $Re_\infty=(10^3-10^4)$ for three $Ra=(10^3, 10^4, 10^5)$ at $\phi=0.08$. It can be noticed from the figure as Re_∞ increases, Nu_{avg} increases and the percentage increment become 6.45% between the lowest and highest Re_∞ values (i.e., $Re_\infty = 10^3-10^4$) at $Ra=10^3$ then the increment reduces to 3.08% at $Ra=10^5$. This behavior attributed to high cooling rate exerted from left cavity wall when compared to buoyancy effect at the lower Ra value (i.e., $Ra=10^3$) which leading to augment the heat transfer rate within the cavity, while the reduction at the increment with the higher Ra (i.e., $Ra=10^5$) belongs to the effect of buoyancy force will be larger than the cooling from left cavity wall and this indicates Re_∞ effect on Nu_{avg} will be higher at the lower Ra .

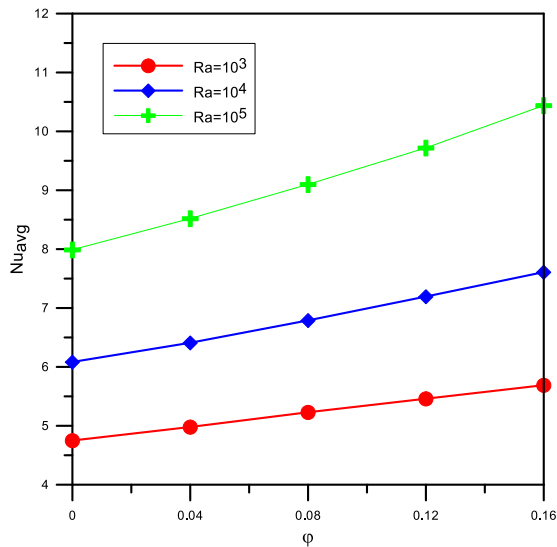


Fig. 9 Average Nusselt number variation versus Cu-water nanofluid volume fraction at bottom wall of cavity with different Rayleigh number at $Re_\infty=10^4$, $Pr_\infty=0.715$

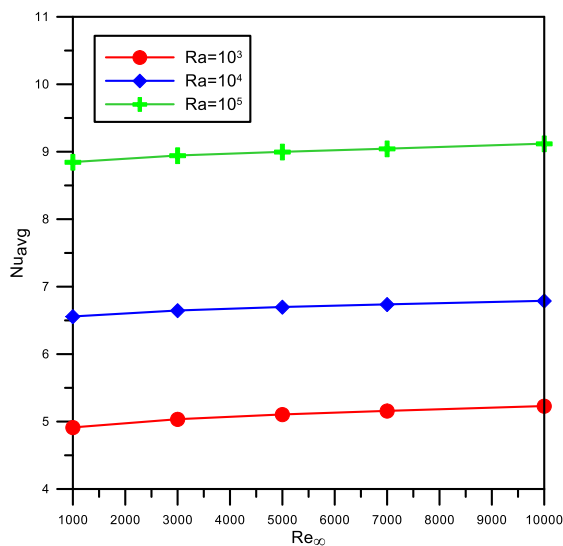


Fig. 10 Average Nusselt Number variation versus air stream Reynolds number with different Rayleigh number at $\phi=0.08$, $Pr_\infty=0.715$

V. CONCLUSIONS

The natural convection flow in a square cavity utilizing Cu-water nanofluid and subjected to cold air stream from left wall has been examined numerically using finite volume scheme. The study has been carried out with taking into account the impact of numerous parameters as nanofluid volume fraction (ϕ), Rayleigh number (Ra) and air stream Reynolds number (Re_∞). The next conclusions can be abridged from the obtained results:

1. Increasing each of nanofluid volume fraction, Rayleigh number and free stream Reynolds number leads to augmenting the heat transfer rate by 30.67% at $\phi=(0-0.16)$, 83.48% at $Ra=(10^3-10^5)$ and 6.45% at $Re_\infty = (10^3-10^4)$ respectively.

2. Generally increases both of nanofluid volume fraction and Rayleigh number will increase the circulation at the core of the cavity.
3. Increasing free stream Reynolds number will increase rate of cooling from left cavity wall and leads to reduce circulation and forming secondary vortices on the cavity.
4. The influence of nanofluid volume fraction will be more prominent at higher values of Rayleigh number.
5. The increment on average Nusselt number with free stream Reynolds number will be more with lower Rayleigh value (i.e., $Ra=10^3$).
6. The flow configuration inside the cavity depends mainly on the relation between buoyancy and rate of air cooling from left wall of the cavity.

VI. REFERENCES

- [1] Alizadeh, M. R. and Dehghan, A.A., "Conjugate natural convection of nanofluids in an enclosure with a volumetric heat source". Arab J. Sci. Eng., 39, 1195–1207, 2014.
- [2] Farooq, G., Leila, J., Mohammad, M. R., Arash, B., and Mohammed, E. A., "Numerical simulation of natural convection of the nanofluid in heat exchangers using a Buongiorno model". App. Math. and Comp., 254, 183-203, 2015.
- [3] Leong, K. Y., Saidur, R., Kazi, S. N., and Mamun, A. H., "Performance investigation of an automotive car radiator operated with nanofluid-based coolants (nanofluid as a coolant in a radiator)". J. Applied Thermal Engineering, 30, 2685-2692, 2010.
- [4] Min, Z., Ruixiang, W., and Jiangfeng, L., "Actuality and application foreground of nanofluids in refrigeration system". Materials Science Forum, 694, 261-265, 2011.
- [5] Xing, L., Ying, C., Songping, M., Lisi, J., and Xuefeng, S., "Effect of surface modification on the stability and thermal conductivity of water-based SiO_2 -coated graphene nanofluid". Thermochemica Acta, 595, 6-10, 2014.
- [6] Manab, K.D., and Pravin, S.O., "Natural convection heat transfer augmentation in a partially heated and partially cooled square cavity utilizing nanofluids". Int. J. Numerical Methods for Heat and Fluid Flow, 19, 411-431, 2009.
- [7] Jahanshahi, M., Hosseinizadeh, S.F., Alipanah, M., Dehghani, A., and Vakilinejad, G.R., "Numerical simulation of free convection based on experimental measured conductivity in a square cavity using Water/ SiO_2 nanofluid". Int. Commun. Heat and Mass Transf., 37, 687–694, 2010.
- [8] Sheikhzadeh, G. A., Arefmanesh, A., Kheirkhah, M. H, and Abdollahi, R., "Natural convection of Cu–water nanofluid in a cavity with partially active side walls". Euro. J. of Mech. B/Fluids, 30, 166-176, 2011.
- [9] Abbasian, A.A., Mazrouei, S., Mahmoodi, M., Ardeshiri, A., and Aliakbari, M., "Numerical study of mixed convection flow in a lid-driven cavity with

sinusoidal heating on sidewalls using nanofluid". Superlattices and Microstructures, 51, 893-911, 2012.

[10] Rahmati, A.R., Sina, N., and Mehrdad, N. B., "Natural convection flow simulation of nanofluid in a square cavity using an incompressible generalized lattice boltzmann method". Defect and Diffusion Forum, 329, 69-79, 2012. [11] Salva, P., and Chamkha, A.J., "An analysis on free convection flow, heat transfer and entropy generation in an odd-shaped cavity filled with nanofluid". Int. Commun. Heat and Mass Transf., 54, 8-17, 2014.

[12] Said, B., M'barek, F., and Hossine, E., "Natural Convection in a Square Cavity Containing a Nanofluid and a Partially-heated Square Block at the Centre". American J. of Heat and Mass Transf., 4, 40-52, 2017.

[13] Brinkman, H.C., "The Viscosity of Concentrated Suspensions and Solutions". J. of Chemical Physics, 20, 571-581, 1952.

[14] Eastman, J.A., Choi, S.U.S., Yu Li, S., Yu W., and Thompson, L.J., "Anomalously increased effective thermal conductivity of ethylene glycol-based nanofluids containing copper nanoparticles". Appl. Phys. Lett., 78, 718-720, 2001.

[15] Jang, S.P., Seok, P., and Choi, S.U.S., "The role of Brownian motion in the enhanced thermal conductivity of nanofluids". Appl. Phys. Lett., 84, 4316-4318, 2004.

[16] Khanafer, K., Kambiz, V., and Marilyn, L., "Buoyancy-driven heat transfer enhancement in a two-dimensional enclosure utilizing nanofluids". Int. J. Heat Mass Transf., 46, 3639-3653, 2003.

[17] Theodore, L.B., Adrienne, S.L., Frank, P.I., and David, P. D., "Fundamentals of heat and mass transfer", seventh ed., John Wiley & Sons Inc, 2011.

[18] Ibtissam, E., and Rachid, S., "Numerical Study of Natural Convection in a Two-Dimensional Enclosure with a Sinusoidal Boundary Thermal Condition Utilizing Nanofluid". Engineering, 4, 445-452, 2012.

[19] Patankar, S.V., "Numerical Heat Transfer and Fluid Flow". First ed., Hemisphere, 1980.

[20] Sathiyamoorthy, M., Tanmay, B., Roy, S., and Pop, I., "Steady natural convection flows in a square cavity with linearly heated side wall(s)". Int. J. Heat Mass Transf., 50, 766-775, 2007.

NOMENCLATURE

Symbol	Description	Units
C_p	Specific heat at constant pressure	J/kg.K
g	Gravitational acceleration	m/s ²
Gr	Grashof Number	–
h	Average convective heat transfer coefficient	W/m ² .K
k	Thermal conductivity	W/m.K
L	Cavity length	m
Nu	Local Nusselt number	–
Nu_∞	Average Nusselt number for air stream	–
p	Pressure	Pa
P	Dimensionless pressure	–
Pr	Prandtl number	–
Ra	Rayleigh number	–
Re_∞	Reynolds number for air stream	–
u, v	Velocity components	m/s
U, V	Dimensionless velocity components	–
U_∞	Free stream velocity	m/s
T	Temperature	K
T_∞	Free stream temperature	K
T_r	Reference temperature	K
x	Axial distance	m
X	Dimensionless axial distance	–
y	Vertical distance	m
Y	Dimensionless vertical distance	–
Greek symbols		
α	thermal diffusivity	m ² /s
β	thermal expansion coefficient	1/K
ψ	stream function	m ² /s
μ	dynamic viscosity	kg/m.s
ν	kinematic viscosity	m ² /s
ω	vorticity	–
ϕ	nanofluid volume fraction	–
ρ	density	kg/m ³
θ	dimensionless temperature	–
Subscripts		
avg	average	
C	cold	
f	fluid	
H	hot	
nf	nanofluid	
s	solid	
∞	free air stream	

VIII. BIOGRAPHY

Khalid Bakir Saleem received his B.Sc. degree in Mechanical Engineering from Dept. of Mechanical Engineering, College of Engineering, University of Basrah, Basrah, Iraq in 1998. He received the M.Sc. degree in “Mechanical Engineering” from University of Basrah, Iraq in 2001 in the field of Thermal Systems-Fluid Mechanics. He also received the Ph.D. degree in “Mechanical Engineering” from University of Basrah, Iraq in 2009 in the fields of Thermal Systems-Multiphase Flows. He worked as a member of teaching staff at the Dept. of Mechanical Engineering, College of Engineering, University of Basrah, Basrah, Iraq from 2002 till present. His research interests in CFD-Nanotechnology-Heat Exchangers-Cavity Flows and Two Phase Flows.